pK_a of the essential Glu54 and backbone conformation for subunit *c* from the H^+-coupled F_1F_0 ATP synthase from an alkaliphilic *Bacillus*

Iván O. Rivera-Torres[a], Ray D. Krueger-Koplin[a], David B. Hicks[b], Sean M. Cahill[a], Terry A. Krulwich[b], Mark E. Girvin[a,*]

[a] *Department of Biochemistry, Albert Einstein College of Medicine, 1300 Morris Park Avenue, Bronx, NY 10461, USA*
[b] *Department of Pharmacology and Biological Chemistry, Mount Sinai School of Medicine, New York, NY 10029, USA*

Received 26 June 2004; revised 30 July 2004; accepted 17 August 2004

Available online 11 September 2004

Edited by Stuart Ferguson

Abstract The conformation of the ATP synthase *c*-subunit and the pK_a of its essential E54 residue were characterized in alkaliphilic *Bacillus pseudofirmus* OF4. The *c*-subunit folds as a helix–loop–helix, with inter-helical contacts demonstrated by paramagnetic relaxation effects. The E54 pK_a of 7.7 is significantly higher than in non-alkaliphiles, which likely prevents proton loss from the *c*-rotor at high pH. The E54 pK_a was unchanged in a mutant, *c*P51A, that has a severe ATP synthesis defect at high pH only. *c*P51 must have some structural role that accounts for the mutant defect, such as different subunit-subunit interactions at high pH.

Keywords: Alkaliphile; Oxidative phosphorylation; Membrane protein; NMR

1. Introduction

Like mitochondria and most other bacteria, extremely alkaliphilic *Bacillus pseudofirmus* OF4 synthesizes ATP using a proton-coupled F_1F_0-ATP synthase. ATP synthases function by a rotary mechanism energized by respiration-dependent proton extrusion [1–4]. This proton extrusion generates an electrochemical proton gradient (Δp) across the coupling membrane that energizes movement of protons through a pathway that is constituted by the membrane-embedded *a*- and *c*-subunits in bacterial synthases. Protons entering through the external side of the *a*-subunit reach the centrally located carboxylates of the hairpin-like *c*-subunits. In different synthases, 10–14 *c*-subunits form an oligomeric ring. Upon protonation of the carboxylates, rotation of the *c*-ring causes rotation of a central $\gamma\varepsilon$-subunit stalk that extends through the core of the hydrophilic F_1 assembly of catalytic subunits. Subsequent conformational changes lead to ATP synthesis. Alkaliphiles like *B. pseudofirmus* OF4 must overcome unique challenges to achieve robust ATP synthesis at pH values $\geqslant$ 10.5 using a proton-coupled ATP synthase [5,6]. At pH 10.5, the pH homeostasis mechanism maintains a cytoplasmic pH of 8.2 in cells growing non-fermentatively on malate, i.e., a large energetically adverse pH gradient [6]. Hence, oxidative phosphorylation by *B. pseudofirmus* OF4 at pH 10.5 occurs at a bulk Δp that is roughly one-third the driving force at pH 7.5. The capture and entry of protons into the synthase, proton movement through the proton path of the synthase, and ultimate proton release into the cytoplasm are challenged by both the actual paucity of protons in the external *milieu* and the low Δp. A final challenge is the threat that upward vicissitudes in external pH will compromise pH homeostasis by allowing proton loss from the cytoplasm through the proton pathway of ATP synthase.

In spite of all these challenges, *B. pseudofirmus* OF4 exhibits a high molar growth yield on malate, and ATP synthesis proceeds to higher phosphorylation potentials at pH 10.5 than pH 7.5 [6], running counter to the chemiosmotic model in which ATP synthesis is directly related to the magnitude of the bulk Δp [7]. Various global adaptations of the cell surface have been suggested to overcome or ameliorate these challenges by proton sequestration at the surface but none of these obviates the need for more specific adaptations [8,9]. Recent studies demonstrate that three special features of the ATP synthase itself are critical for oxidative phosphorylation by *B. pseudofirmus* OF4 at pH 10.5 but not at pH 7.5 [9,10]. These alkaliphile-specific features are: two sequence features in the *a*-subunit that abut or are within the putative proton uptake pathway; and an "extra proline" in the *c*-subunit, *c*P51. This proline is on the cytoplasmic side of the key carboxylate (*c*E54) which has another, conserved proline (*c*P57) on its periplasmic side. The extra proline is only found in extreme alkaliphiles that grow optimally at pH 10 and above [9,11]. Apart from its role in ATP synthesis, a modest role of *c*P51 and larger roles for two *a*-subunit features are suggested in cytoplasmic proton retention during a sudden shift of cells to pH 10.5 media [9]. The presence of several alkaliphile-specific features in the alkaliphile *c*-subunit, including the proline at *c*-51, raised the possibility that the alkaliphile *c*-subunit has structural adaptations that optimize its interplay with its alkaliphile-specific *a*-subunit or have other roles in overcoming the energetic challenges of proton-coupled ATP synthesis at high pH [9]. To understand the structural roles of these alkaliphilic-specific sequence variations in ATP synthesis at high external pH, we are undertaking structural characterization of the *c*-subunits from

* Corresponding author. Fax: +1-718-430-8565.
E-mail address: girvin@aecom.yu.edu (M.E. Girvin).

0014-5793/$22.00
doi:10.1016/j.febslet.2004.08.049

wild-type and mutant *B. pseudofirmus* OF4. Here, we report the secondary structure of the wild-type protein, and the pK_as of the essential E54 side chain in both the wild-type and P51A mutant subunits.

2. Materials and methods

2.1. Expression, purification, and sample preparation

Wild-type and P51A and I59C mutant *B. pseudofirmus* OF4 subunits *c*, cloned into the pET-3 vector, were overexpressed in *Escherichia coli* strain C43(DE3) [12] grown on minimal M63 media with $^{15}NH_4Cl$ and ^{12}C-glucose or $^{15}NH_4Cl$ and ^{13}C-glucose as the nitrogen and carbon sources. The proteins were extracted from cells with chloroform/methanol (2:1) and precipitated with diethyl ether [13]. The *B. pseudofirmus* OF4 subunit was separated from a minimal amount of background wild-type *E. coli* subunit *c* either by Sephadex LH60 chromatography using 50 mM ammonium acetate in 1:1 $CHCl_3$:CH_3OH, or by anion exchange HPLC (AX300 column, eluted with an ammonium acetate gradient in 4:4:1 $CDCl_3$:CD_3OH:H_2O; [14]). A Sephadex LH20 column in 1:1 $CHCl_3$:CH_3OH was subsequently used to remove the ammonium acetate. Except where noted, NMR samples were 1.5 mM ^{15}N or $^{13}C^{15}N$-labeled protein in 600 μl of 4:4:1 $CDCl_3$:CD_3OH:H_2O, 25 mM d_{11}-Tris, pH 7.8, prepared as described [15,16].

2.2. Backbone resonance assignments

All NMR experiments were performed at 303 K on a Bruker DRX-600 spectrometer. NMR data were processed using NMRpipe [17] and analyzed using NMRView [18]. The pH and sample stability were monitored by comparing ^1H and $^1H^{15}N$ HSQC spectra before and after flame sealing the NMR tube, and between 3D NMR experiments. Wild-type backbone resonance assignments were obtained from the following 3D experiments: $^1H^{15}N$ NOESY-HSQC, $^1H^{13}C$ NOESY-HSQC, $^1H^{15}N$ TOCSY-HSQC, $^1H^{15}N$ HNHA, CBCANH, CBCA (CO)NH, HNCO, HCCH-TOCSY, and HCCH-COSY [19,20].

2.3. Nitroxide spin labeling and data analysis

Quantitative spin-label modification of 20 mg of the I59C mutant protein was performed prior to purification by reaction with 6 mM (maleimidomethyl)-PROXYL in 5 ml of 2:1 $CHCl_3$:CH_3OH, for 120 min at 25 °C. The modified protein was purified and separated from excess reagent by LH60 and LH20 chromatography. The completeness of modification was confirmed spectrophotometrically. NMR samples were ~0.5 mM ^{15}N-labeled protein in 600 μl of 4:4:1 $CDCl_3$:CD_3OH:H_2O, 25 mM d_{11}-Tris, pH 7.8. After collecting a 2D $^1H^{15}N$ HSQC data set on the paramagnetic sample, the PROXYL group was reduced by addition of 6 μl of 400 mM phenylhydrazine in 4:4:1 $CDCl_3$:CD_3OH:H_2O at pH 7.8 and a second HSQC data set was collected. Cross-peak intensities were measured in the paramagnetic (oxidized) and diamagnetic (reduced) spectra. The intensities for the reduced sample were scaled by a factor of 0.8, empirically determined to minimize the differences in intensities of the least affected signals between the two samples. The ratios of intensities (oxidized over reduced) were calculated for all cross-peaks. Residues less than 18 Å from the spin label were identified by intensity ratios less than 0.7 [21].

2.4. pH titrations

The titration behaviors of protonatable residues in the wild-type and the P51A mutant were monitored using 2D $^1H^{15}$HSQC NMR spectra. Samples of *B. pseudofirmus* OF4 subunit *c* were 0.5–1 mM ^{15}N-labeled protein in 600 μl of 4:4:1 $CDCl_3$:CD_3OH:H_2O, 10 mM ammonium acetate, 10 mM MES, 10 mM Tris, and 10 mM CAPS. Tetramethylsilane was added as internal reference. The pH was varied from 2.9 to 9.75 by addition of NH_4OH or HCl. The pH and NMR sample stability were monitored by direct pH measurement, and by recording 1D ^1H spectra before and after each 2D $^1H^{15}N$ HSQC experiment. Sample stability was severely compromised in samples either prepared or adjusted to a pH above 9.75. Each 2D $^1H^{15}N$ HSQC data set was collected as 128 t_1 increments of 8 transients each. To determine the pK_a for E54, its ^1H and ^{15}N chemical shifts as a function of pH were fit to the modified Henderson–Hasselbalch equation:

$$\delta = \delta_{prot} + [(\delta_{de} - \delta_{prot})/1 + 10^{(pH-pK_a)}] \quad (1)$$

where δ is the chemical shift at a given pH, δ_{prot} and δ_{de} are the chemical shifts limits of the fully protonated and deprotonated residues, respectively [22].

3. Results

3.1. Backbone resonance assignments

The $^1H^{15}N$ HSQC spectrum of wild-type *B. pseudofirmus* OF4 subunit *c* shows that most of the amide cross-peaks were resolved (Fig. 1A). A total of 65 amides were visible in the $^1H^{15}N$ HSQC spectrum at pH 7.8. Exceptions were the amide corresponding to the N-terminal methionine, visible only below pH 6.0, and the three proline residues (P36, P51, and P57). Periodic collection of this spectrum showed that the sample remains stable for several months in this solvent mixture after flame sealing the NMR tube.

A series of 3D NMR experiments on ^{15}N and $^{13}C^{15}N$-labeled wild-type OF4 subunit *c* samples were used to assign the C_α, C_β, CO, H_α, H_β and H_N spins, and measure backbone NOEs and coupling constants at pH 7.8. The patterns of $d_{NN(i,i\pm1)}$, $d_{\beta N(i,i+1)}$, and medium range NOEs (Fig. 1B), secondary shifts of backbone resonances (Fig. 1C–E), and $^3J_{HNH\alpha}$ coupling constants (Fig. 1F) were all characteristic of α-helical secondary structural elements [23] extending from residue 2–31 in the N-terminal transmembrane segment, and from residue 37–69 in the C-terminal segment, with a short loop connecting the two helices.

3.2. Inter-helical contacts from PROXYL labeled I59C

Because of the chemical shift degeneracy typically encountered in helical membrane proteins, long range inter-helical NOEs can be difficult to identify unambiguously (e.g., [16]). An unpaired electron in paramagnetic groups, such as nitroxides, induces significant proton relaxation enhancements, which provide distance measurements of up to 20 Å that are useful for protein structural studies [21,24,25]. To determine whether the two helices observed for *B. pseudofirmus* OF4 subunit *c* associated stably with each other, we used the (maleimidomethyl)-PROXYL nitroxide spin label to modify a Cys substituted at position 59 in the C-terminal helix. A 2D $^1H^{15}N$ HSQC spectrum was collected on the sample with the PROXYL in its paramagnetic state, and a second control HSQC spectrum was collected after quantitative reduction of the nitroxide to its diamagnetic form. Since paramagnetic relaxation from an introduced nitroxide spin label leads to distance-dependent broadening, it is most conveniently measured as a decrease in cross-peak intensity [21,25]. The relaxation effects on all subunit *c* amide protons are plotted as intensity ratios (paramagnetic/control) in Fig. 2. As expected, cross-peaks corresponding to residues 52–60, and 63, 64, and 68, which neighbor C59 in the C-terminal helix, were weak or absent in the spectrum of the paramagnetic sample. After reduction of the nitroxide, all cross-peaks were again observed in the $^1H^{15}N$ HSQC spectrum. Several cross-peaks for N-terminal residues (I8, A9, and A10) were also extremely weak in the paramagnetic sample, indicating contact between the N- and C-terminal helices. The pattern of effects implied an interaction between the two helices, with residue 59 in the C-terminal helix located opposite to residue 9 in the N-terminal helix.

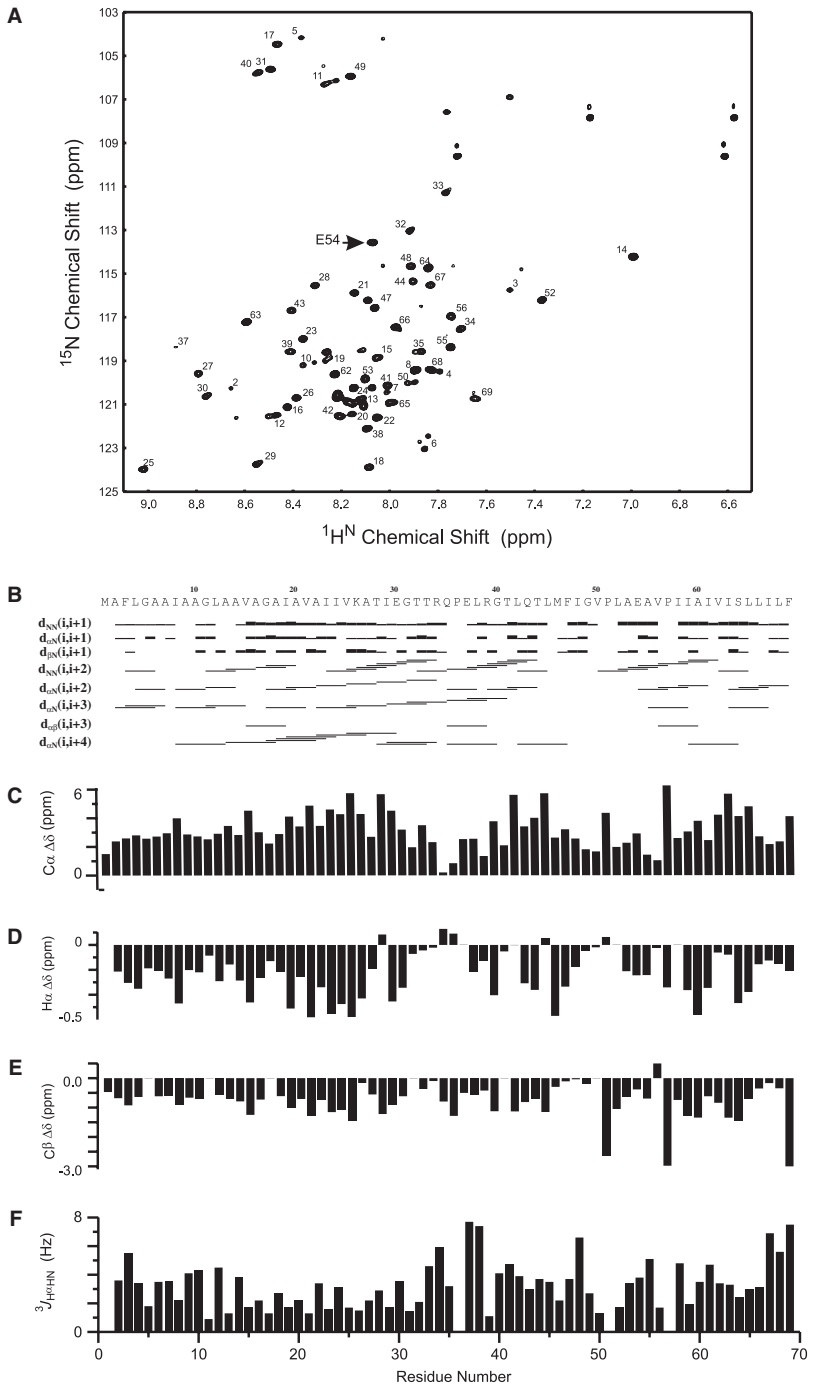

Fig. 1. NMR spectrum and structural parameters for wild-type *B. pseudofirmus* OF4 subunit *c*. (A) $^{1}H^{15}N$ HSQC spectrum at pH 7.8 with assigned amide resonances labeled. (B) Backbone NOE pattern observed in 3D NOE data sets. (C–E) Deviations of chemical shifts from random coil values are plotted for Cα (C), Hα (D), and Cβ (E). (F) HN–Hα coupling constants, measured in a 3D HNCA-*J* experiment.

3.3. E54 pK_as for wild-type and P51A mutant subunit c

Changes in the NMR chemical shifts of a protonatable residue as a function of pH can readily be used to measure its pK_a. A pH titration in the *E. coli* subunit *c* monitored by 2D $^{1}H^{15}N$ HSQC spectra showed that the backbone amide resonance with the most extensive chemical shift changes corresponded to Asp61 (unpublished data). We followed the chemical shift changes of all assigned amides over a pH range of 3–9.75 to define the titration behavior of the acidic and basic residues of wild-type and P51A mutant *B. pseudofirmus* OF4 subunit *c*. The *B. pseudofirmus* OF4 subunit *c* sequence contains three acidic and three basic residues. As expected, the largest chemical shift changes from pH 6–9 were observed for the essential, proton-translocating E54. The ^{15}N frequencies of the wild-type and P51A mutant shifted by 1.4 ppm and 1.1 ppm, respectively, on raising the pH from pH 6–9. Fitting the E54 chemical shift changes to Eq. (1) gave pK_a values of 7.74 and 7.67 for the wild-type and P51A mutant proteins in mixed

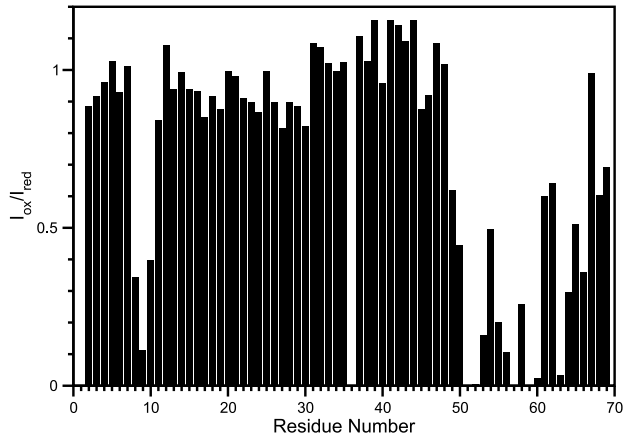

Fig. 2. Relaxation effects on backbone amides from site specific spin-labeling at residue 59. The relaxation effects are shown as intensity ratios (paramagnetic over control) for each non-proline residue in *B. pseudofirmus* OF4 subunit *c* at pH 7.8. In addition to large effects on residues adjacent to the spin-labeling site in the C-terminal helix, significant paramagnetic relaxation was observed for residues 8–10 in the N-terminal helix.

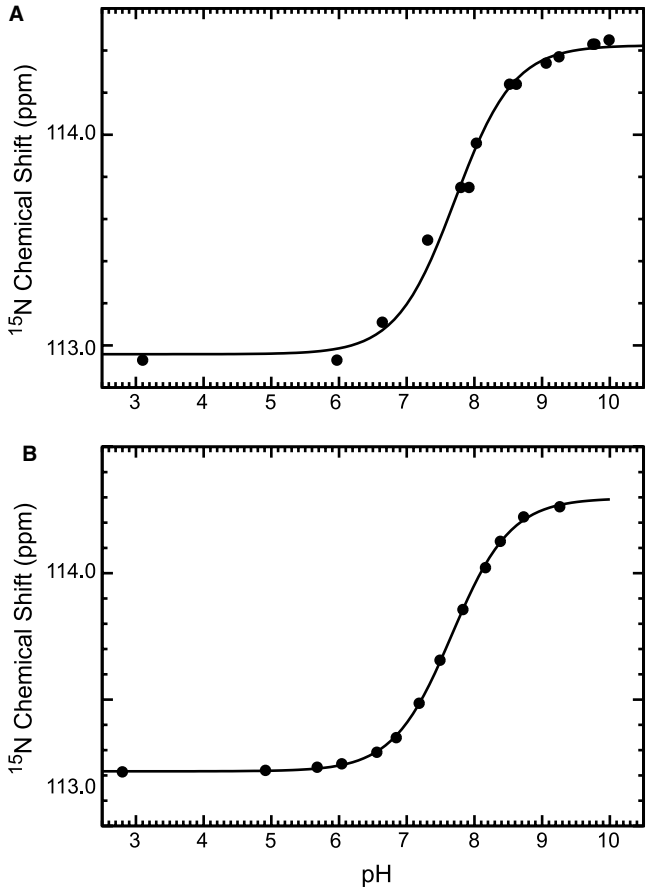

Fig. 3. Titration of E54 pK_as. (A) Plot of ^{15}N chemical shifts for E54 of wild-type subunit *c* versus pH. The best fit of the modified Henderson–Hasselbalch equation to the data, giving a pK_a of 7.74 is plotted as a solid line. (B) pH titration of the P51A mutant subunit *c* plotted as above, but with the best fit giving a pK_a of 7.67.

organic solvents (Fig. 3). The two other acidic side chains, E30 and E37, titrated with pK_a values of 4.8 and 5.3, respectively. The amplitude and pattern of chemical shift changes versus residue number over the pH range of 6–9 were similar to those previously reported for the *E. coli* subunit [26]. No evidence for any additional conformational changes above the pK_a of E54 was observed.

4. Discussion

pK_a *of E54*. The pK_a for the essential E54 in wild-type *B. pseudofirmus* OF4 subunit *c* was measured to be 7.74. This is almost 3 pH units higher than the pK_a values for E30 and E37, the other two acidic residues in the protein. The local structure around E54 has clearly been optimized to raise the pK_a to the physiological range, and these structural features are preserved in the monomeric subunit in 4:4:1 $CHCl_3$:CH_3OH:H_2O mixed solvent. The pK_a of E54 is also significantly higher than both the equivalent D61 in *E. coli* subunit *c*, which was measured to be 7.1 under identical solution conditions [27] and estimated to be near pH 7 in the F_1F_0 complex [28], and the equivalent E65 in *P. modestum* subunit *c*, measured indirectly to be 7.0 in the absence of Na^+ using detergent solubilized F_1F_0 [29]. While one might have predicted a larger increase in pK_a, to some value between the pH_{in} of 8.2 and the pH_{out} of 10.5 of alkaline growth conditions, the E54 pK_a increase of 0.6–0.7 for this facultative alkaliphile is probably a necessary compromise. The pK_a must be both low enough to support the release of protons from the *c*-rotor towards a cytoplasm at pH 7.5 during growth at near-neutral pH and simultaneously high enough to accept protons from their site of entry into F_0 during growth at high pH.

The *c*P51A mutant has same pK_a as the wild-type, within experimental error. While the P51A substitution had profound effects on ATP synthesis at high pH, only a hint of proton loss relative to wild type was observed [9], consistent with the equivalence of their pK_a values. The extremely deleterious effect of the mutation on non-fermentative growth and respiration-dependent ATP synthesis at pH 10.5 may result from altered interactions with the specially adapted alkaliphilic subunit *a* that result in inefficient local coupling under high pH conditions. The equivalent *c*G58 in the *E. coli* subunit lies on the face of the C-terminal helix that packs against subunit *a*, as shown by cross-linking experiments [30] and the resulting structural model for the subunit *a*–*c* interface [31]. Alternatively, the P51 of wild-type *B. pseudofirmus* OF4 subunit *c* might have a role in *c*-subunit packing that facilitates an unusual *c*-subunit stoichiometry; this stoichiometry could be altered in the P51A mutant and in turn affect the energetics of oxidative phosphorylation at high pH [2].

Since the assignments and structural constraints were obtained at a pH value near the pK_a of E54, it is not possible to define the 3D structure of the subunit from these data, because the subunit would be exchanging between protonated and deprotonated conformations. However, we can conclude that the secondary structure is an N-terminal helix extending from residues 2–31, connected by a short loop (residues 32–36) to a C-terminal helix extending from residues 37–65. Deviations in backbone chemical shifts from their random coil values and $^3J_{HNH\alpha}$ coupling constants did indicate the possibility of a break in the C-terminal helix at G49, near P51. Unlike the *c*-

subunit from *P. modestum* where no evidence for long range contacts between helices was observed [16], the spin label data demonstrate that the subunit does adopt a tertiary fold in mixed solvents, with contact between the N- and C-terminal helices as had been observed for the *E. coli* subunit [15]. The paramagnetic relaxation effects of the spin label at residue 59 on the amides of I8–A10 are quite consistent with the structure of the *E. coli* subunit [15], where the equivalent I66 lies across the inter-helical interface from the equivalent residues V15–M17. Hence, the isolated *B. pseudofirmus* OF4 subunit *c* gives every indication of adopting a stable tertiary structure, which merits more complete structural study above and below the pK_a of E54.

pH-dependent conformational changes. The amplitudes and sequence distribution of the chemical shift changes for backbone resonances in the *B. pseudofirmus* OF4 subunit on going from pH 6 to pH 9 are similar to those seen for the *E. coli* subunit in mixed solvents [26]. Hence, one would expect to find conformational changes in *B. pseudofirmus* OF4 subunit *c* on changing protonation state of E54 that are similar to those observed for the *E. coli* subunit [31]. However, no evidence for additional conformational changes was observed at higher pH. Hence, the proposed "gating" conformational change in facultative alkaliphiles that switches between proton access to the external media and some kind of sequestered acquisition of protons does not originate in subunit *c* [8,32]; subunit *a* is the more likely gating site, as indicated by a recent study [9] in which *a*K180G and *a*G212S mutants exhibit a 10-fold increase in ATP synthesis relative to wild type by ADP + Pi-loaded vesicles in response to an imposed (bulk) diffusion potential at high pH, in addition to increased hydrolytic activity of the ATPase and increased proton loss to the bulk upon an alkaline shift in pH_{out} [9].

Acknowledgements: This research was supported by grants GM55371, GM28454, PF-00-343-01-GMC, and T32 CA09060. Instrumentation was supported by NSF 9601607 and the Howard Hughes Medical Institute.

References

[1] Stock, D., Leslie, A.G. and Walker, J.E. (1999) Science 286, 1700–1705.
[2] Stock, D., Gibbons, C., Arechaga, I., Leslie, A.G.W. and Walker, J.E. (2000) Curr. Opin. Struct. Biol. 10, 672–679.
[3] Fillingame, R.H., Angevine, C.M. and Dmitriev, O.Y. (2003) FEBS Lett. 555, 29–34.
[4] Tsunoda, S.P., Aggeler, R., Yoshida and Capaldi, R. (2001) Proc. Natl. Acad. Sci. USA 98, 898–902.
[5] Hicks, D.B. and Krulwich, T.A. (1990) J. Biol. Chem. 265, 20547–20554.
[6] Sturr, M.G., Guffanti, A.A. and Krulwich, T.A. (1994) J. Bacteriol. 176, 3111–3116.
[7] Mitchell, P. (1961) Nature 191, 144–148.
[8] Krulwich, T.A. (1995) Mol. Microbiol. 15, 403–410.
[9] Wang, Z., Hicks, D.B., Guffanti, A.A., Baldwin, K. and Krulwich, T.A. (2004) J. Biol. Chem. 279, 26546–26554.
[10] Ivey, D.M. and Krulwich, T.A. (1992) Res. Microbiol. 143, 467–470.
[11] Keis, S., Kaim, G., Dimroth, P. and Cook, G.M. (2004) Biochim. Biophys. Acta 1676, 112–117.
[12] Miroux, B. and Walker, J.E. (1996) J. Mol. Biol. 260, 289–298.
[13] Fillingame, R.H. (1976) J. Biol. Chem. 251, 6630–6637.
[14] Hermolin, J. and Fillingame, R.H. (1989) J. Biol. Chem. 264, 3896–3903.
[15] Girvin, M.E., Rastogi, V.K., Abilgaard, F., Markley, J.L. and Fillingame, R.H. (1998) Biochemistry 37 (25), 8817–8824.
[16] Matthey, U., Braun, D. and Dimroth, P. (2002) Eur. J. Biochem. 269, 1942–1946.
[17] Delaglio, F., Grzesiek, S., Vuister, G.W., Zhu, G., Pfeifer, J. and Bax, A. (1995) J. Biomol. NMR 6, 689–707.
[18] Johnson, B.A. and Blevins, R.A. (1994) J. Biomol. NMR 4, 603–614.
[19] Cavanagh, J., Fairbrother, W.J., Palmer III, A.G. and Skelton, N.J. (1996) Protein NMR Spectroscopy: Principles and Practice. Academic Press, San Diego, CA.
[20] Grzesiek, S. and Bax, A. (1993) J. Biomol. NMR 3, 185–204.
[21] Battiste, J.L. and Wagner, G. (2000) Biochemistry 39, 5355–5365.
[22] Dwek, R. (1973) Nuclear Magnetic Resonance in Biochemistry. Oxford University Press, Glasgow.
[23] Wüthrich, K. (1986) NMR of Proteins and Nucleic Acids. Wiley, New York, NY.
[24] Girvin, M.E. and Fillingame, R.H. (1994) Biochemistry 33, 665–674.
[25] Yu, L., Meadows, R.P., Wagner, R. and Fesik, S.W. (1994) J. Magn. Reson. Series B 104, 77–80.
[26] Rastogi, V.K. and Girvin, M.E. (1999) J. Biomol. NMR 13, 91–92.
[27] Assadi-Porter, F.M. and Fillingame, R.H. (1995) Biochemistry 34, 16186–16193.
[28] Zhang, Y. and Fillingame, R.H. (1994) J. Biol. Chem. 269, 5473–5479.
[29] Kluge, C. and Dimroth, P. (1993) Biochemistry 32, 10378–10386.
[30] Jiang, W. and Fillingame, R.H. (1998) Proc. Natl. Acad. Sci. USA 95, 6607–6612.
[31] Rastogi, V.K. and Girvin, M.E. (1999) Nature 402, 263–268.
[32] Guffanti, A.A. and Krulwich, T.A. (1994) J. Biol. Chem. 269, 21576–21582.